

# Effects of O addition on the thermal behaviour of hard W–N sputtered coatings

C. Louro\*, J.C. Oliveira, A. Cavaleiro

SEG-CEMUC, Mechanical Engineering Department, University of Coimbra, Polo II, 3030-788 Coimbra, Portugal

## A B S T R A C T

### Keywords:

Tungsten oxynitride  
Sputtering  
Thermal behaviour  
HT-XRD  
Hardness

The structural thermal behaviour of three W–O–N sputtered coatings with similar metalloid to metal ratio ( $\sim 2.1$ ) was investigated up to 900 °C after annealing in a vacuum tube furnace as well as *in-situ* HT-XRD under a controlled atmosphere of Ar–5% $H_2$ . The as-deposited microstructure of the coatings consisting in a nanocomposite of low-order W–O and W–N phases evaluated differently as a function of the oxygen content. The W–O–N film containing more than 27 at.% O delaminated severely from the steel substrates for temperatures as low as 500 °C. In opposite, for the coatings with less O content, the low range order of the as-deposited structure was maintained up to 800 °C and with further annealing crystallized into a mixture of  $WO_2$  and  $W_2N$ . The thermal behaviour of the oxynitride films overcame that observed for oxygen-free nitride ones. This is due to the greater N content retaining during annealing treatment, in opposite to the W–N films which give rise to the single metallic  $\alpha$ -W phase. The structural and compositional evolution supported the hardness behaviour obtained by the thermal treatment in protective ambiance.

© 2009 Elsevier Ltd. All rights reserved.

## 1. Introduction

Important research work has been conducted on transition metal nitrides (TM–N), owing to their excellent mechanical properties, in order to develop these materials as hard and wear-resistant coatings, to be applied, e.g., for increasing the performance of cutting tools based on cemented carbides and high speed steel materials. Nevertheless, some of them, due to their low oxidation threshold temperature as well as their structural instability originated by  $N_2$  liberation, may have limited applications for wear resistance at elevated temperatures. Such is the case of the W–N sputtered system. Previous studies revealed that tungsten nitride could reach outstanding mechanical (hardness  $\sim 40$  GPa) and tribological properties (wear rates  $< 0.5 \times 10^{-6}$  mm<sup>3</sup>/Nm) [1]. However, the study of its tribological behaviour at high temperatures [2] showed a considerable performance decrease due to their low oxidation resistance, which set-point temperature was fixed only at  $\sim 600$  °C [3,4].

One of the possibilities to overcome this drawback would be the addition of oxygen to the W–N coatings. The final scope would be favouring the formation of a thin top protector W–O layer and, thus, the delaying of the oxidation process. However, the O contents have to be optimized in order not to degrade the intrinsic mechanical and tribological properties of the tungsten nitride phases, as was

demonstrated previously [5]. In this study, therefore, three tungsten oxynitride coatings with similar metalloid–metal ratio ( $((O + N)/W \sim 2.1)$ ) were deposited by reactive magnetron sputtering. Thermal treatments up to 900 °C were conducted in protective environment to investigate the O effect on the compositional, structural and mechanical behaviour of the W–O–N films. The idea is to contribute for the understanding of the thermal behaviour of sputtered W-based coatings in order to interpret future research results on oxidation resistance, where complex interactions of temperature changes and oxygen-rich ambiance attack are simultaneously present.

## 2. Experimental details

W–O–N films were produced by d.c. reactive magnetron sputtering, using the aforementioned procedure [5]. The coatings, with thickness in the range 2.5–3.5  $\mu$ m, were deposited onto Fecralloy substrates (Goodfellow). An oxygen-free nitride film was also deposited to be used as a reference sample having an impurity content level less than 2 at.% O.

The annealing studies were carried out under protective Ar–5% $H_2$  atmosphere in a vacuum tube furnace (after evacuation less than  $10^{-3}$  Pa) between 400 and 800 °C during 30 min as well as in a High Temperature X-ray Diffractometer (HT-XRD). The *in-situ* XRD analysis were performed in a vacuum chamber HT16 under continuous Ar–5% $H_2$  flux at low pressure ( $1^{-10}$  Pa) after evacuating the chamber down to a value lower than  $10^{-3}$  Pa. The chamber is

\* Corresponding author.

E-mail address: [cristina.louro@dem.uc.pt](mailto:cristina.louro@dem.uc.pt) (C. Louro).

couple to a Philips X'Pert diffractometer. All the analysis were done with Co radiation ( $K_{\alpha} = 0.178897$  nm) in Bragg-Brentano geometry. The samples ( $12 \times 10$  mm) were fixed on a Pt plate and heated from RT up to  $900^{\circ}\text{C}$  in steps of  $100^{\circ}\text{C}$ . The heating rate was  $40^{\circ}\text{C}/\text{min}$  between each temperature step followed by maintenance of  $\sim 20$  min for XRD acquisition in  $25\text{--}65^{\circ}$  range. The samples were cooled down to RT and new XRD patterns were acquired.

The elemental composition of the films was analysed by Electron Probe Microanalysis (Cameca SX-50), whereas the mechanical properties (hardness) were evaluated by ultramicroindentation (Ficherscope H100) with a Vickers indenter by applying a nominal load of 20 mN in both as-deposited and post-annealing state. Each hardness value is a result of at least ten indentation tests. The hardness results were corrected in relation to the geometrical defects of the indenter, the thermal drift and the uncertainty in zero position [6].

### 3. Results and discussion

#### a) As-deposited coatings

Table 1 summarises the main characteristics of the as-deposited sputtered coatings as well as those related to the W–N reference sample. During this work the coatings will be denoted as is ascribed in Table 1.

In respect to the as-deposited structure, Fig. 1 shows the X-ray diffraction patterns obtained for the films under study. All the W–O–N films exhibit broad and low intensity X-ray diffraction peaks in comparison to  $W_{42}N_{58}$  coating, this effect being more pronounced as higher as the O content is. The formation of low-order arrangement structures could be attributed on the one hand to the very small crystallite size of the films. Due to the too low substrate temperature ( $\sim 350^{\circ}\text{C}$ ) not sufficient to allow the crystallisation process, and, on the other hand, to the competitive growth of different structures that can coexist in the W–O–N system: binary oxides ( $WO_x$ ) and nitrides (WN,  $W_2N$ ) as well as oxynitrides ( $W_x(O,N)_{1-x}$ ) phases. In fact, the constant presence of two different broad peaks in the region of  $2\theta \in [25\text{--}45^{\circ}]$  suggests that the coatings have a nanocomposite structure containing simultaneously tungsten nitride and oxide phases (two zones marked in Fig. 1). For example, for the  $W_{32}O_{24}N_{44}$  film, the three broad peaks centred at  $2\theta$  of  $40.9$ ,  $49.5$  and  $73.5^{\circ}$  fit quite well to the (111), (200) and (220) reflections of cubic  $\beta$ - $W_2N$  phase [ICDD 25-1257], respectively. The indexed bcc  $\alpha$ -W [ICDD 04-0806] is related to the interlayer used to improve the adhesion of the ternary coatings to the steel substrates (no adhesion interlayer was used for the reference sample). The presence of the  $\beta$ -W [ICDD 47-1319] structure, currently denoted as the  $W_3O$  phase, should be also attributed to the adhesion interlayer being its formation due to the absorption of O from the reactive process by the metallic W interlayer.

The structure of the reference  $W_{42}N_{58}$  sample is in agreement with that obtained previously [4,7]; for N contents higher than

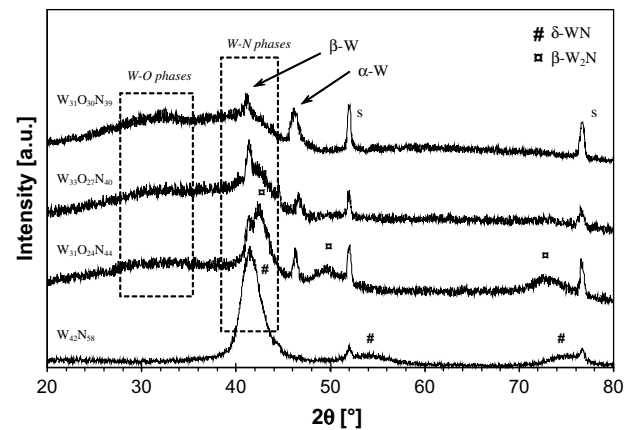


Fig. 1. X-ray diffraction patterns of the as-deposited W–N and W–O–N coatings.

55 at.%, the W–N films crystallise into the hexagonal  $\delta$ -WN phase [ICDD 25-1256] with a (100) preferential orientation.

Tungsten nitride is known as a hard coating presenting hardness values in the range of 30–41 GPa [5,7]. However, when oxygen is sputter added to W–N system the hardness significantly drops down to values in the range of 15–30 GPa. This hardness decline is much more evident as the amount of the W–O phase increases in relation to W–N phase [5]. Similar hardness values as those presented in the Table 1 have already been observed in other transition oxynitride systems [8–10]. From the previous studies [5] on the mechanical properties of the W–O–N system it was shown that the addition of oxygen was only effective for improving the hardness values if an increase of the internal stress of the coatings occurred simultaneously.

#### b) Thermal stability

Fig. 2 presents the structural evolution with increasing annealing temperature of the coatings treated in a tube furnace. Diffraction patterns of the W–O–N films containing less than 27 at.% O reveal no significant changes in either the relative peak intensity or in the peak position up to  $500^{\circ}\text{C}$  (Fig. 2a) and b)), suggesting that the as-deposited short-range order structures are retained after annealing. Conversely, the XRD patterns of the coatings with higher O contents show that at  $400^{\circ}\text{C}$  the metastable  $\beta$ -W phase starts to transform into  $\alpha$ -W in agreement with its well-known thermal instability [11]. Furthermore, for the highest O containing film,  $W_{31}O_{30}N_{39}$ , the thermal treatment at  $500^{\circ}\text{C}$  gives rise to a severe mechanical instability leading to the coating detachment from the steel substrate after cooling down to RT (see the insert optical micrograph in Fig. 2a)). As can be observed in this figure besides the intense and well defined diffraction peaks of the steel substrate, the other two can be indexed as the  $\alpha$ -W and  $\beta$ -W phases, related with the adhesion interlayer. For temperatures higher than  $600^{\circ}\text{C}$ , Fig. 2b), the XRD peaks of the oxynitride coatings containing respectively 24 and 27 at.% O, become narrower, more intense and shifted to equilibrium positions, features characteristic of the structural recovery and the grain growth. Taking into account the  $2\theta$  peaks position, the values of the interplanar distance obtained after peak fitting match quite well with either  $\beta$ - $W_2N$  or  $W_x(O,N)_{1-x}$  [ICDD 25-1254] phases. In fact, due to the similarity on the peaks position of these two phases, both from the cubic system, it is impossible to assign which one should be present, keeping the doubt about the possibility of existence of O atoms in the  $W_2N$  lattice. Thermal treatments higher than  $700^{\circ}\text{C}$  give rise to the crystallisation of the amorphous W–O phase, as  $WO_2$  [ICDD 86-0134], enhancing

Table 1  
Characteristics of the as-deposited W–O–N sputtered films.

Film	Thickness ( $\mu\text{m}$ )	Composition (at.%)			Metalloid/metal (atomic ratio)	Hardness (GPa)
		W	O	N		
$W_{42}N_{58}$	2.9	40.7	1.30	58.0	1.4	$23.7 \pm 1.1$
$W_{32}O_{24}N_{44}$	2.5	31.5	24.1	44.4	2.2	$20.5 \pm 1.3$
$W_{33}O_{27}N_{40}$	2.5	32.9	27.1	40.0	2.1	$11.5 \pm 0.5$
$W_{31}O_{30}N_{39}$	3.5	31.1	30.2	38.7	2.2	$11.4 \pm 0.9$

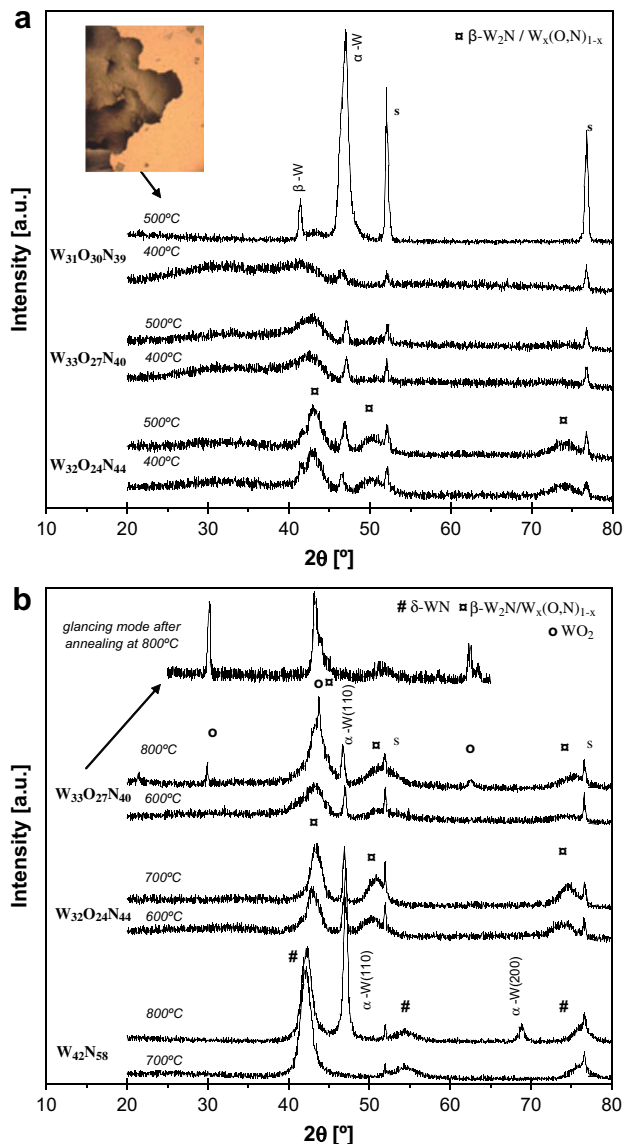


**Fig. 2.** Structural evolution of the W–O–N coatings thermally treated in a tube furnace under protective atmosphere between a) 400–500 °C (optical micrograph of the post-annealed  $W_{31}O_{30}N_{39}$  film at 500 °C is present as inset); and b) 600–800 °C annealing temperature (includes the XRD glancing mode of the  $W_{33}O_{27}N_{40}$  film after annealed at 800 °C).

the phase separation referred to above for the nanocomposite structure (for example  $W_{33}O_{27}N_{40}$  film in Fig. 2b)).

*In-situ* XRD analysis of the 24 at.% O containing film confirms the annealing tube furnace results, although a little delayed with temperature. As can be seen in Fig. 3a), no important structural changes in the coating are detected, the as-deposited low-order arrangement being thermally stable with increasing annealing temperature up to 800 °C. At 900 °C the crystallisation process of the W–O amorphous phase starts to occur. The formation of tungsten oxide phase,  $WO_2$ , is detected with narrow XRD peaks suggesting a much higher grain size than the one characteristic of the other phases, the  $\beta$ - $W_2N$  and/or the  $W_x(O,N)_{1-x}$ , that continues to be indexed at the highest temperatures tested. For highest temperature, in the case of oxygen-free sample, the W–N phase starts to transform as it can be concluded by the analysis Fig. 2b). *In-situ* HT-XRD of this film (Fig. 3b)) shows that at 600 °C precipitation of  $\alpha$ -W phase starts to occur (small peak at  $\sim 46.5^\circ$  – it is worthy

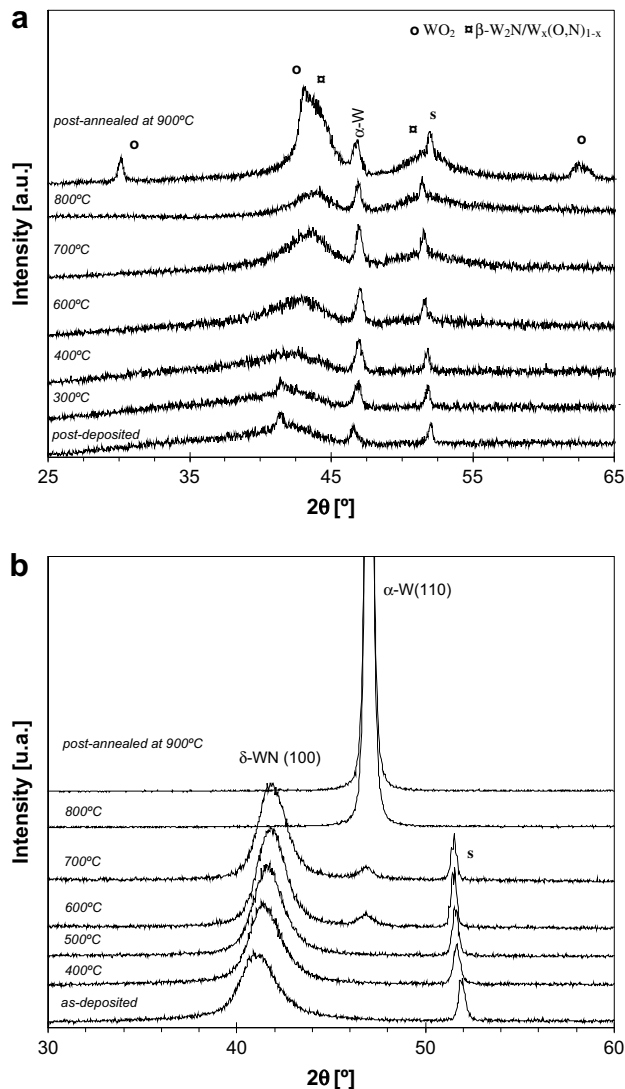


**Fig. 3.** *In-situ* HT-XRD structural evolution of the a)  $W_{33}O_{27}N_{40}$  and b)  $W_{42}N_{58}$  coatings annealed in protective atmosphere ( $Ar-5\%H_2$ ) up to 900 °C.

noting that this coating was deposited without adhesion interlayer) whose intensity grows with annealing temperature at the expenses of the  $\delta$ -WN phase. Such a trend coincides with the progressive loss of N in W–N film, which almost vanishes for temperatures higher than 800 °C. This structural instability was also stated in previous research works [12,13] and could only be avoided if a nitrogen-containing atmosphere is used during heat treatments [14].

On the other hand, for W–O–N coatings, in spite of some N losses (Fig. 4), the final content at 800 °C are still enough to support the detection of the  $W_2N$  phases at this temperature (e.g., the composition is  $W_{39}O_{39}N_{22}$  for the as-deposited  $W_{33}O_{27}N_{40}$ ). Thus, these observations reveal that the thermal stability of W–O–N films, containing O less than 27 at.%, is better compared to single-phase W–N coatings, since the nitride phase is observed at higher annealing temperature.

The higher thermal stability of the  $W_2N$  phases in the oxynitride coatings was proposed to be associated to either the formation of an O-rich over-layer, or the enrichment of  $W_2N$  grain boundaries by oxygen atoms, both impeding the outward N effusion during annealing [15]. In authors' opinion, the first suggestion seems to be more suitable since the narrow XRD peaks of the oxide phase indicate a grain size not compatible with the second alternative.

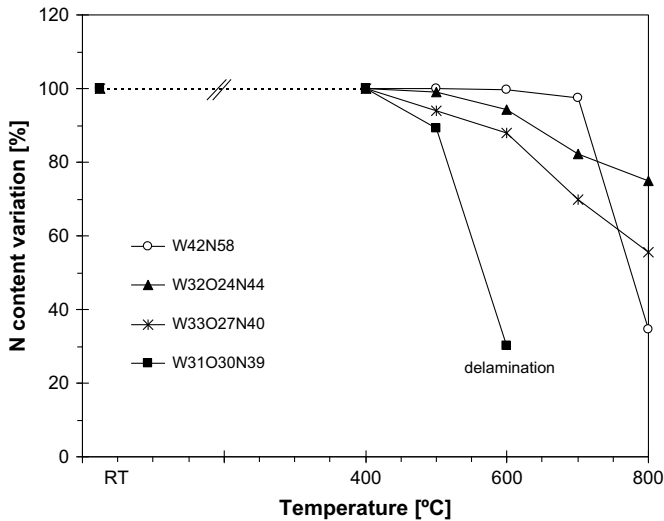


Fig. 4. Evolution of the nitrogen content (normalised to the as-deposited value) with increasing annealing temperature.

Fig. 2b) shows the XRD patterns of the  $W_{33}O_{27}N_{40}$  coating post-annealed at 800 °C in glancing mode (2°). It is obvious the enhancement of the intensities of the XRD peaks assigned to the  $WO_2$  phase when tested by this XRD geometry, confirming that the sample surface forming these continuous oxide layer is more reliable.

The results of the evaluation of the hardness after annealing at increasing temperatures are shown in Fig. 5. Up to 600 °C no significant changes are detected in the hardness values excepting the sudden decreases observed for  $W_{31}O_{30}N_{39}$  film at 500 °C, probably related to the delamination already referred to above. The small increase observed for the W–O–N coating with increasing annealing temperature, can be explained by the progressive diminution of the  $\beta$ -W ( $W_3O$ ) which, as demonstrated in previous works

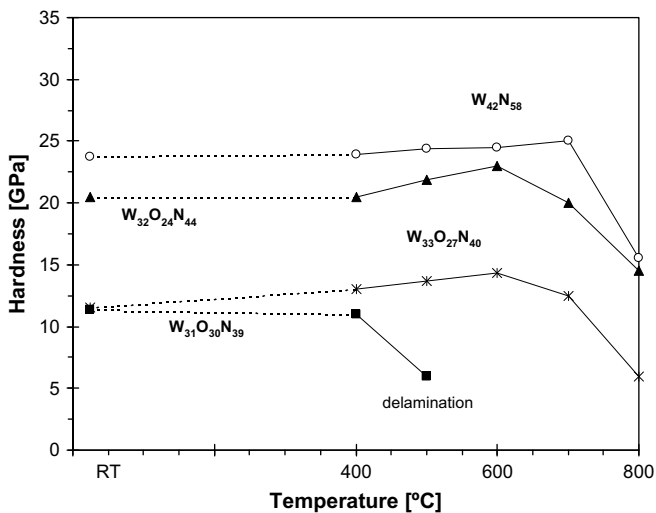


Fig. 5. Hardness evolution of the W–O–N coatings evaluated after cooling from increasing annealing temperature.

[5] is the softest phase in the W–N sputtered system. The hardness drops observed for temperatures higher than 600 °C confirm the statements above discussed, i.e., in the case of W–O–N coatings the formation of the top oxide layer and, for W–N film, the loss of the N content and the formation of the metallic  $\alpha$ -W phase. In fact, authors previous works [5] showed that: i) oxide phases are generally softer than nitride ones which explain that during nanoindentation measurements, as the depth maintains quite small (~300 nm) the top oxide layer will contribute for a lower measured hardness; ii)  $\alpha$ -W coatings has lower hardness than W–N coatings, particularly when deposited with low compressive stress levels.

#### 4. Conclusions

This study has shown that the annealing process at temperatures up to 900 °C, under protective atmosphere, can strongly influence the structure, the chemical composition and the mechanical properties of nanocomposite sputtered tungsten oxynitride coatings.

In general, the lower the O content the better the thermal behaviour of W–O–N films was. For O contents higher than 27 at.% the films spall off severely for temperatures as low as 500 °C. The films with lower O content were more thermally stable than the oxygen-free nitride one used as reference. At 800 °C, after crystallisation as  $WO_2 + W_2N$  mixture, the nitride phase remained stable whereas it almost vanished in W–N film due to N outwards effusion. It was proposed that such behaviour could be associated to the formation of an O-rich over-layer, impeding the N loss.

As a consequence of the annealing process, a progressive improvement in the hardness behaviour is reached up to 600 °C followed by a decrease for higher temperatures. This behaviour was explained in the light of the crystallisation process.

#### Acknowledgements

The authors are gratefully acknowledged the financial supported of this work by the European Union through the NMP3-CT-2003-505948 “HARDECOAT” project and FCT through REVDUR-POCI/V.5/A037/2005.

#### References

- [1] Polcar T, Parreira NMG, Cavaleiro A. *Wear* 2007;262:655–65.
- [2] Polcar T, Parreira NMG, Cavaleiro A. *Wear* 2008;265:319–26.
- [3] Louro C, Cavaleiro AC. *J Electrochem Soc* 1997;144:259–64.
- [4] Cavaleiro C, Louro C, Montemor F. *Surf Coat Technol* 2000;131:441–7.
- [5] Parreira MG, Carvalho NJ, Vaz F, Cavaleiro A. *Surf Coat Technol* 2006;200:6511–6.
- [6] Antunes JM, Cavaleiro A, Menezes LF, Simões MI, Fernandes JV. *Surf Coat Technol* 2002;149:27–35.
- [7] Louro C, Cavaleiro A. *Surf Coat Technol* 1999;116–119:121–7.
- [8] Vaz F, Carvalho P, Cunha L, Rebouta L, Moura C, Alves E, et al. *Thin Solid Films* 2004;469–470:11–7.
- [9] Fenker M, Kappl H, Tetrikowski K, Bretzler R. *Surf Coat Technol* 2005;200:1356–60.
- [10] Banakha O, Heulin T, Schmid PE, Le Dréo H, Tkalec I, Levy F, et al. *J Vac Sci Technol* 2006;A 24(2):1–6.
- [11] Wagner RS, Sinha AK, Sheng TT, Levinstein HJ, Alexander FB. *J Vac Sci Technol* 1974;11(3):582–7.
- [12] Reid JS, Kolawa E, Ruiz RP, Nicolet MA. *Thin Solid Films* 1993;236:319–24.
- [13] Shen YG, Mai YW, McBride WE, Zhang QC, McKenzie DR. *Thin Solid Films* 2000;372:257–64.
- [14] Ferreira L, Louro C, Cavaleiro A, Trindade B. *Key Eng. Mater.* 2002;230/232:640–3.
- [15] Shen YG, Mai YM. *Mat Sci Eng* 2000;B76:107–15.